ACS APPLIED MATERIALS & INTERFACES

Research Article

Cite This: ACS Appl. Mater. Interfaces XXXX, XXX, XXX−XXX

www.acsami.org

Friction Modulation via Photoexcitation in Two-Dimensional Materials

Xiaofei Liu,* Yao Li, and Wanlin Guo*

State Key Laboratory of Mechanics and Control of Mechanical Structures, Key Laboratory for Intelligent Nano Materials and Devices of Ministry of Education, Nanjing University of Aeronautics and Astronautics, Nanjing 210016, China

Supporting Information

ABSTRACT: We demonstrate a photoexcitation-friction coupling in bilayered black phosphorus, a two-dimensional semiconductor crystallized via van der Waals interaction, using density functional theory and the Prandtl−Tomlinson model. Under an experimentally accessible electron−hole density of 5×10^{13} cm^{-2}, the energy barrier for interlayer sliding can be reduced by 13% and the resultant reduction of critical force for stick−slip transition can be up to 4.7%. With the carrier density being doubled, the frictional anisotropy can even be eliminated. Analysis based on Born−Oppenheimer approximation shows that photoexcitation-friction coupling can be universal for van der Waals crystals with interlayer electronic states responsive to both photoexcitation and interlayer sliding.

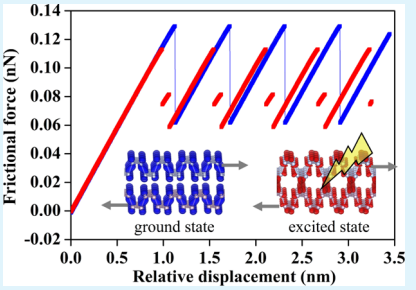

KEYWORDS: *black phosphorus, photoexcitation, friction, optomechanical coupling, density functional theory*

1. INTRODUCTION

Friction, a common mechanical phenomenon in daily life, can resist relative sliding of moving bodies, dissipate kinetic energies of mechanical systems, and wear materials in contact.[1,2] Although low friction is often desirable for reducing energy loss and wear, high friction can be required as for automobile tires and brakes, underscoring the importance of friction control. Strategies used to modulate friction rely on changing the physical or chemical properties of the interface. This is often achieved by changing shape and roughness of surfaces in contact or using lubricating oil.[3−5] Additionally, modification of interfacial commensurability, surface chemical functionalization, isotopic effects of phonons, and even electric field-induced charge traps can be useful.[6−10]

The interaction at an interface without chemical bonding is determined jointly by electrostatic forces and van der Waals (vdW) forces. Thus, modification of interfacial electronic states would be a straightforward way to control friction. A question then naturally arises: could photo illumination that can excite electronic states in semiconductors from the highest occupied molecular orbital (HOMO) into the lowest unoccupied molecular orbital (LUMO) be used for friction control? Few-layered vdW crystals offer a natural platform to answer this question. On the one hand, vdW crystals such as graphite, MoS_2, and h-BN are crystallized by interlayer vdW interactions[11−14] and they have long been used as solid lubricants.[15−17] On the other hand, their ultrathin nature allows the excited carriers to be concentrated at the interface.

In this work, we show by first-principles simulations and the Prandtl−Tomlinson model that photoexcitation can modulate the interlayer friction in bilayered black phosphorus. The energy barrier of the periodic surface potential can be reduced by 13% under an excited electron−hole (e−h) density of 5×10^{13} cm^{-2} and resultantly the critical force for onset of the interlayer slip can be reduced by 4.7%. With the e−h density being doubled, the frictional anisotropy in bilayered black phosphorus can be eliminated. The underlying mechanism for the photoexcitation-friction coupling is understood from the Born−Oppenheimer approximation.

2. COMPUTATIONAL DETAILS

To quantitatively investigate the coupling between photoexcitation and interlayer friction in bilayered black phosphorus, the periodic surface potentials were calculated using first-principles simulations. The ground-state (GS) electronic structure and energy were solved with the standard density functional theory (DFT).[18] To deal with the electronic excitation stimulated by the linearly polarized light, the Δ-self-consistent-field (ΔSCF) method formulated by Görling was applied.[19] Both calculations for ground and excited states were performed with the ABINIT code,[20] using the optimized norm-conserving Vanderbilt pseudopotential.[21] The generalized gradient approximation of the Perdew−Burke−Ernzerhof functional was used for the exchange correlation potential.[22] The Grimme's DFT-D2 approach was applied for vdW energy correction,[23] as its results for bulk black phosphorus are in good agreement with quantum Monte Carlo simulations and experimental results.[24] In each sliding position, the atomic structure was allowed to relax in the normal z direction but the coordinates in the in-plane x, y directions were fixed. It should be noted that the Bethe−Salpeter approach[25] would be more sophisticated for simulation of optical excitation, but it is too

Received: November 8, 2019
Accepted: December 19, 2019
Published: December 19, 2019

DOI: 10.1021/acsami.9b20285
ACS Appl. Mater. Interfaces XXXX, XXX, XXX−XXX

expensive for this study. Nevertheless, the ΔSCF method has faithfully reproduced the photostriction of $BiFeO_3$ observed in experiments and it recently predicted a large photostriction effect in two-dimensional group-IV monochalcogenide.[26,27]

3. RESULTS AND DISCUSSION

The black phosphorus monolayer consists of puckered six-membered rings arranged in tetragonal cells with adjacent zigzag chains being pulled up and down alternately.[28,29] A characteristic of phosphorus is that each P atom has a single lone pair, which in conjunction with three P−P bonds forms the sp^3 hybridization.[30] Peculiar to the friction of bilayered phosphorus is that the lone pairs are localized in the interlayer region, thus influencing the surface potential. As shown by DFT calculations in Figure 1, the lone pairs contribute to both

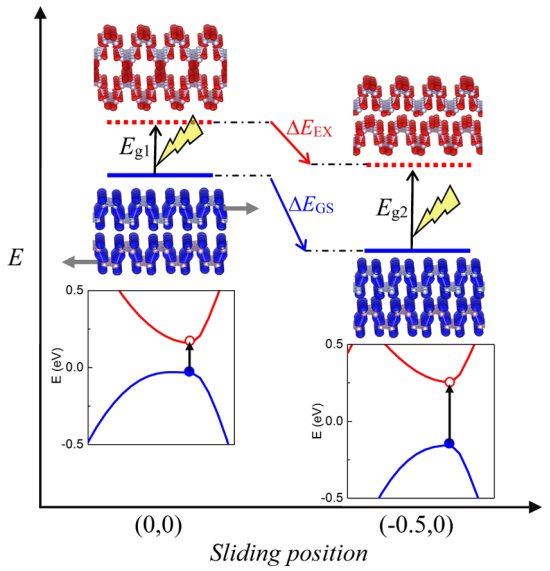

Figure 1. Illustration for the evolution of HOMO and LUMO energy levels and charge distributions in bilayered black phosphorus at the eclipsed stacking position (0,0) and staggered stacking position (−0.5,0). The solid and dotted lines stand for the total electron-ion energies of the bilayer in the ground and excited states, respectively. E_{g1} and E_{g2} denote the bandgap at the two sliding positions.

the HOMO and LUMO in bilayered black phosphorus. Another feature of bilayered black phosphorus is its linear dichroism: a sharp absorption peak in the visible region can be stimulated by incident light polarized along the armchair direction, but for light polarized along the zigzag direction, an absorption peak appears at a higher energy level.[31] Importantly, the HOMO−LUMO transition corresponding to the sharp absorption peak appears regardless of the detailed stacking mode, as illustrated in Figure 1 or reported in a previous work.[32]

Figure 2a shows the contour plot of surface potential for the interlayer sliding of bilayered black phosphorus without photo illumination. The surface potential has a tetragonal primitive translational cell, in which four high-symmetric sliding positions that have two mirror axes along the x and y directions are labeled by the coordinates (0,0), (0,−0.5), (−0.5,0), and (−0.5,−0.5) in unit of the basis vectors a, b (see the stacking modes in Figure 2). The sliding positions (0,0) and (−0.5,−0.5) are the hills of potential because of the eclipsed stacking and resultant large interlayer exchange repulsion. The position (−0.5,0) with a staggered stacking manner is a global basin of potential. The staggered position (0,−0.5) is a saddle point instead, whereas another local minimum locates at the low-symmetric staggered position (±0.202,0.5).

We assume that the excited e−h density in the sliding bilayer black phosphorus was 5×10^{13} cm^{-2}, a value experimentally accessible for two-dimensional crystals.[33] The photoexcitation in the ΔSCF calculations is realized by exciting a fraction of states from the HOMO into LUMO. Specifically, states at four k-points around the Brillouin zone center out of a 9×12 mesh are excited. Upon the photoexcitation, the hills and basins of surface potential are not substantially shifted from the original positions. However, the energy barriers are remarkably modulated (Figure 2b). For example, the energy differences between the excited and GSs are 33 and 55 meV at (0,0) and (−0.5,0), respectively, thus reducing the barrier height along the path (−0.5,0)−(0,0) by 13.3%. When the e−h density is doubled, the original saddle point (0,−0.5) turns to be a local basin, being lower in energy than (±0.202,0.5).

The interlayer sliding in bilayered black phosphorus belongs to the scope of atomic-scale friction, characterized by atomic-scale stick−slip processes.[34−36] As illustrated in Figure S1, an atomistic layer is subjected to the surface potential of another atomistic layer underneath and pulled by an elastic spring. Within the one-dimensional Prandtl−Tomlinson model,[37,38] the total potential energy of the mechanical system reads $V = E(d) + \frac{1}{2}k(d - D)^2$, where E is the surface potential and k and D stand for the stiffness of the spring and the displacement of the moving support connected with the spring, respectively. When the spring is not sufficiently stretched, the top layer can reside in a local minimum of total potential energy and slid forward smoothly or it is said to be in the stick regime. As the local minimum turns unstable during sliding, the top layer will suddenly slip to another stable minimum. The equation of force equilibrium $F = \frac{\partial E}{\partial d} = k(d - D)$ then can be used to derive the borderlines between the stick and slip regimes.

For a macro center-of-mass motion of the top layer, the micro sliding pathway usually follows one-dimensional MEPs of the surface potential. Figure 2a−c shows the MEPs in the ground and excited states searched with a string method.[39] Two inequivalent MEPs are found for the GS: path I passing through (−0.5,0), (−0.202,−0.5), (0.202,−0.5), and (0.5,−1) and path II passing through (−0.5,0), (−0.202,−0.5), and (−0.5,−1). With an e−h density of 5×10^{13} cm^{-2}, the pathways are slightly disturbed. However, the potential energy along the MEPs that determines the micro stick−slip processes is significantly modulated by the photoexcitation (Figure 2d). The height of the energy barrier between the local basins (±0.202, 0.5) along path I is reduced from 29 to 2 meV and the energy of the two hills along path II is also reduced. When the e−h density is doubled, the pathways I and II become equivalent, with the barrier between the local basins (±0.202, 0.5) being eliminated.

Figure 3a,b presents the numerical results for the interlayer friction along paths I and II derived by a spring with a stiffness of 0.5 meV/Å^4. Without photoexcitation, the lateral force exhibits a typical sawtooth behavior. The force first increases linearly and then drops suddenly, showing a stick−slip transition within a single sliding periodicity. The forces for the onset of slip along paths I and II are measured to be 0.129

DOI: 10.1021/acsami.9b20285
ACS Appl. Mater. Interfaces XXXX, XXX, XXX−XXX

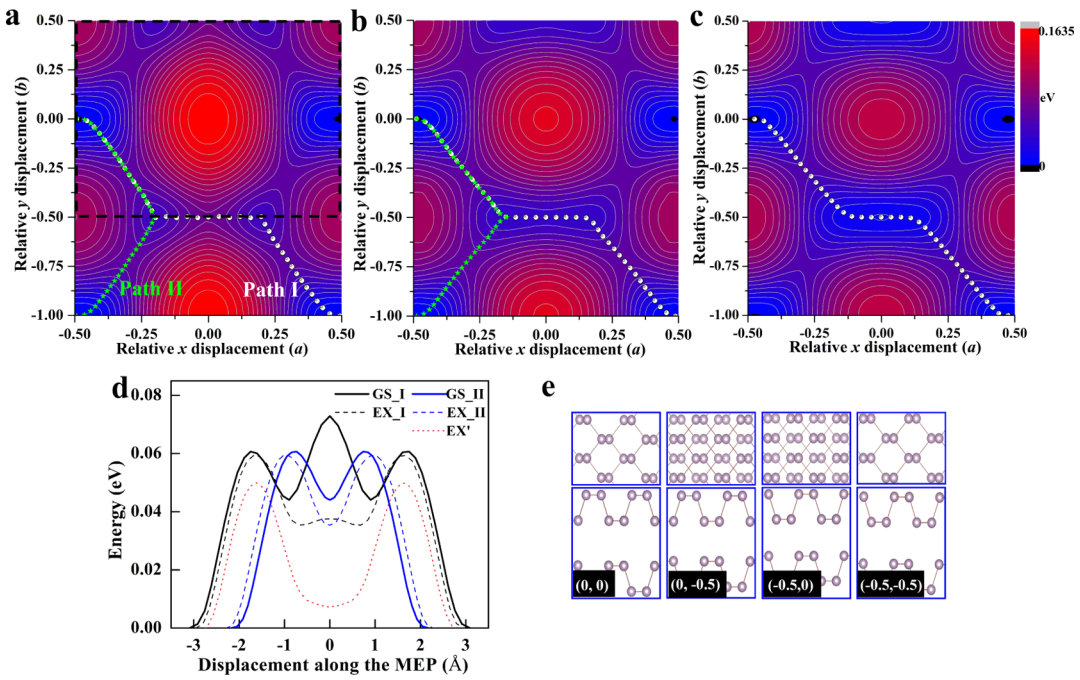

Figure 2. Surface potential for interlayer sliding in bilayered black phosphorus at (a) the GS, (b) the excited state with an e−h density of 5×10^{13} cm^{-2} (EX), and (c) the excited state with an e−h density of 1×10^{14} cm^{-2} (EX′). The displacements are in unit of the basis vectors. The primitive cell of the periodic surface potential is labeled by dotted black lines in (a). The circles and stars denote the minimum energy paths (MEPs) I and II, respectively. Only one of the two equivalent MEPs is shown in (c). (d) Potential energies along the MEPs. The global minimums are set as the zero energy. (e) Atomic structures of bilayered black phosphorus at the high-symmetric positions of the surface potential.

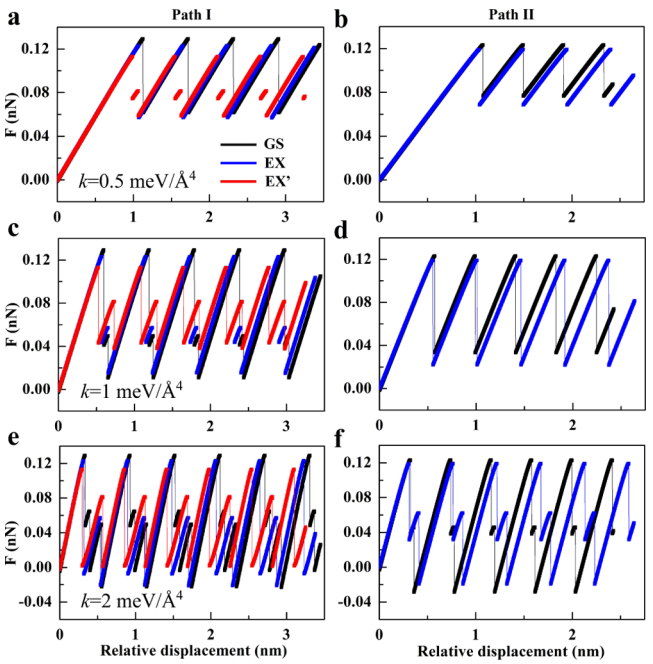

Figure 3. Lateral force acting on the sliding layer as a function of the displacement of moving support. The friction curves at the GS, EX, and EX′ states are plotted with the black, blue, and red colors, respectively. The left (a,c,e) and right (b,d,f) panels correspond to the frictions along paths I and II, respectively. For the EX′ state, only the results for path I are presented. From the top to bottom panels, the stiffness of the pulling spring is 0.5, 1, and 2 meV/Å^4, respectively.

and 0.123 nN, respectively. As the macro motion along the zigzag direction can follow either path I or II but that along the armchair direction can only follow path I, the different critical forces suggest a frictional anisotropy, complying with the recent experimental measurement using an atomic force microscope (AFM).[40]

Under an e−h density of 5×10^{13} cm^{-2}, the critical forces along paths I and II turn out to be 0.123 and 0.119 nN, respectively. Compared with that in the GS, the photoexcitation leads to a reduction of critical force by 4.7 and 3.3%. With respect to energy dissipation, the work done by the moving support along path I is reduced by 7.7%, owing to the reduced force. However, the work along path II is increased by 4.0% because of the increased sliding distance. When the e−h density is doubled, the critical force can be further reduced to 0.114 nN. Most astonishing is that the friction in the anisotropic black phosphorus turns to be isotropic because paths I and II become equivalent. Another point to be noted is that the sliding layer no longer directly slips to the minimum in the next periodicity. Instead, it first slips to a new minimum within the original periodicity, which is easy to understand as the highest hill of potential transforms to a local minimum upon the photoexcitation.

To test the robustness of the observed effect, friction curves under an elastic spring with different stiffness are shown in Figure 3c−f. It is obvious that the photoexcitation-friction coupling always exists regardless of the spring used. However, the stick−slip behaviors can be influenced by the stiffness of the spring. For the sliding in the dark along path I derived by a spring with a stiffness of 0.5, 1.0, and 2.0 meV/Å^4, there is a single-, double-, and triple-slip within a sliding periodicity, respectively. As the stiffness is increased to 40 meV/Å^4 (Figure S2c,d), the friction evolves into a continuous sliding without the stick−slip process. The evolution of the stick−slip process as a function of stiffness is also sensitive to photoexcitation. With an e−h density of 5×10^{13} cm^{-2}, the friction can change from single-slip to double-slip and then to continuous sliding.

DOI: 10.1021/acsami.9b20285
ACS Appl. Mater. Interfaces XXXX, XXX, XXX−XXX

The phase diagrams in Figure S3 show the stick−slip process under different excitation conditions.

Compared with the well-known photostriction effect, the photoexcitation-friction coupling in bilayered black phosphorus is in fact pronounced. Previously reported photo-induced strain in bulk samples is within the range of 10^{-5} to 10^{-4},[41] much smaller than the ratio of frictional force reduction here. For the recently predicted large photostriction in the SnS monolayer, the photo-induced strain can be up to $\sim -2.5 \times 10^{-3}$ under an e−h density of 4×10^{12} cm^{-2}.[27] Assuming a liner scaling between photo-induced strain and carrier density, the photo-induced strain is in the same order of magnitude as the ratio of reduced frictional force. Although the modulation of frictional force is less significant than that achieved by other methods such as changing the layer number,[42] the photoexcitation-friction coupling exhibits unique advantages. First, this effect can control friction without contacting the sliding body with an agent such as AFM tip. Second, the modulation of friction by photoexcitation is reversible. Third, none of the previous methods can transform an anisotropic friction to be isotropic.

The description of atomic-scale friction with the Prandtl−Tomlinson model is based on the Born−Oppenheimer approximation,[43] assuming that the relaxation of electrons is much faster than the motion of ions and the evolution of electronic states in turn contributes to the potential on ions. Employing the Hellmann−Feynman theorem, the interlayer lateral force can be derived as $F = \frac{\partial E}{\partial d} = \left\langle \Psi_d \middle| \frac{\partial H}{\partial d} \middle| \Psi_d \right\rangle$, where both the stationary many-body wave Ψ_d and the Schrödinger Hamiltonian H are sliding-position-dependent. Within the framework of DFT,[44] the change of force under photoexcitation contains a term

$$\Delta F = \left\langle \Psi_{\mathrm{LUMO}} \middle| \frac{\partial H}{\partial d} \middle| \Psi_{\mathrm{LUMO}} \right\rangle - \left\langle \Psi_{\mathrm{HOMO}} \middle| \frac{\partial H}{\partial d} \middle| \Psi_{\mathrm{HOMO}} \right\rangle \approx \frac{\partial(\varepsilon_{\mathrm{LUMO}} - \varepsilon_{\mathrm{HOMO}})}{\partial d}$$

indicating that few-layered vdW crystals with a sliding position-dependent bandgap would exhibit photoexcitation-tunable frictional properties.

To verify the abovementioned mechanism, we plot the interlayer distance and bandgap as a function of sliding position (Figure 4a,b). The profile of the interlayer distance complies with the surface potential, implying that the exchange repulsion between interlayer electronic states determines the potential. Meanwhile, Figure 4b shows that the variation trend of the bandgap as a function of sliding position along the path (0,0)−(0.5,0) complies with that of the energy difference between the ground and excited states. It is then evident that, as the total electron-ion energy is shifted upward upon photoexcitation, ΔE also changes during sliding because of the modified interactions between interfacial lone pairs, giving rise to the photoexcitation-friction coupling. The influence of vdW interaction can be excluded because the effect of electronic excitation on the interlayer distance is negligible (Figure S4).

The Born−Oppenheimer approximation is valid for the electron-ion systems in electronic GSs. Its application here for the excited system can also be rationalized because we assume a constant and steady e−h density. Without this assumption, the photoexcitation-friction coupling could also be possible. The lifetime of excitons of black phosphorus in room temperature was estimated to be ∼249 ps,[45] being shorter than a stick period (10^{-6} to 10 s) by orders of magnitude.[46] Supposing that the friction is in the stick regime with a lateral force lower than the critical force in the dark but is already higher than that required for slip under photoexcitation, photo illuminations will trigger a slip ahead of the usual slip point. In fact, the previously predicted photostriction effect and the funnel effect of excitons rely on the same approximation.[27,47]

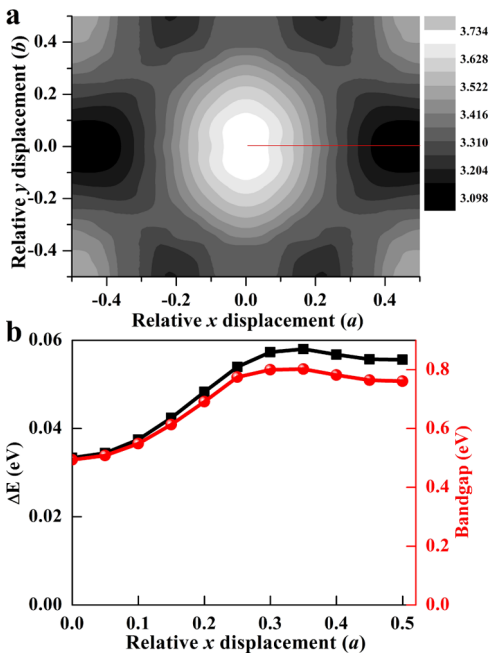

Figure 4. (a) Interlayer distance of bilayer black phosphorus in the GS as a function of sliding position. (b) Energy difference between the EX and GS states and the direct bandgap along the path (0,0)−(0.5,0) shown by the red line in (a).

4. CONCLUSIONS

In conclusion, we demonstrate a photoexcitation-friction coupling in bilayered black phosphorus using first-principles calculations and the Prandtl−Tomlinson model. This new optomechanical coupling originates from the charge redistribution modulated interlayer interaction and it can be applied to control interlayer friction. According to the Born−Oppenheimer approximation, this effect would be significant in vdW crystals with interlayer electronic states simultaneously sensitive to photo illumination and interlayer sliding. For instance, this effect would be weak in bilayered MoS_2 in which the direct bandgap is not sensitive to interlayer sliding[48,49] but it could be strong in bilayered graphyne with stacking-dependent electronic structures.[50] The revealed photoexcitation-friction coupling is not only a novel method for friction control but also crucial to functionality of vdW crystals as candidate materials for future nanoelectromechanical devices.[51−55]

■ ASSOCIATED CONTENT

Supporting Information

The Supporting Information is available free of charge at https://pubs.acs.org/doi/10.1021/acsami.9b20285.

Schematic representation of the Prandtl−Tomlinson model; lateral force acting under a pulling spring with a stiffness of 5 and 40 meV/Å^4; phase diagrams of stick−

DOI: 10.1021/acsami.9b20285
ACS Appl. Mater. Interfaces XXXX, XXX, XXX−XXX

slip regimes as a function of excitation condition and stiffness of the pulling spring; interlayer distances along the path (0,0)−(0.5,0); and details of numerical calculations (PDF)

AUTHOR INFORMATION

Corresponding Authors

*E-mail: liuxiaofei@nuaa.edu.cn (X.L.).
*E-mail: wlguo@nuaa.edu.cn (W.G.).

ORCID

Xiaofei Liu: 0000-0003-0563-3600
Wanlin Guo: 0000-0001-6665-6924

Notes

The authors declare no competing financial interest.

ACKNOWLEDGMENTS

This work is supported by the National Natural Science Foundation of China (11702132, 51535005). X.L. is grateful to the support from the China Postdoctoral Science Foundation (nos. 2016M600408 and 2017T100362) and the Natural Science Foundation of Jiangsu Province (no. BK20170770).

REFERENCES

(1) Bhushan, B.; Israelachvili, J. N.; Landman, U. Nanotribology: Friction, Wear and Lubrication at the Atomic Scale. *Nature* **1995**, *374*, 607−616.
(2) Müser, M. H.; Urbakh, M.; Robbins, M. O. Statistical Mechanics of Static and Low-Velocity Kinetic Friction. *Advances in Chemical Physics*; Wiley, 2003; Vol. *126*, p 187.
(3) Komvopoulos, K.; Choi, D.-H. Elastic Finite Element Analysis of Multi-Asperity Contacts. *J. Tribol.* **1992**, *114*, 823−831.
(4) Berman, D.; Deshmukh, S. A.; Sankaranarayanan, S. K. R. S.; Erdemir, A.; Sumant, A. V. Macroscale Superlubricity Enabled by graphene Nanoscroll Formation. *Science* **2015**, *348*, 1118−1122.
(5) Sulek, M. W.; Kulczycki, A.; Malysa, A. Assessment of Lubricity of Compositions of Fuel Oil with Biocomponents Derived from Rape-Seed. *Wear* **2010**, *268*, 104−108.
(6) Liu, Z.; Yang, J.; Grey, F.; Liu, J. Z.; Liu, Y.; Wang, Y.; Yang, Y.; Cheng, Y.; Zheng, Q. Observation of Microscale Superlubricity in Graphite. *Phys. Rev. Lett.* **2012**, *108*, 205503.
(7) Dag, S.; Ciraci, S. Atomic Scale Study of Superlow Friction between hydrogenated Diamond Surfaces. *Phys. Rev. B* **2004**, *70*, 241401.
(8) Cannara, R. J.; Brukman, M. J.; Cimatu, K.; Sumant, A. V.; Baldelli, S.; Carpick, R. W. Nanoscale Friction Varied by Isotopic Shifting of Surface Vibrational Frequencies. *Science* **2007**, *318*, 780−783.
(9) Park, J. Y.; Ogletree, D. F.; Thiel, P. A.; Salmeron, M. Electronic Control of Friction in Silicon PN Junctions. *Science* **2006**, *313*, 186.
(10) Qi, Y.; Park, J. Y.; Hendriksen, B. L. M.; Ogletree, D. F.; Salmeron, M. Electronic Contribution to Friction on GaAs: An Atomic Force Microscope Study. *Phys. Rev. B: Condens. Matter Mater. Phys.* **2008**, *77*, 184105.
(11) Carter, J. L.; Krumhansl, J. A. Band Structure of Graphite. *J. Chem. Phys.* **1953**, *21*, 2238−2239.
(12) Yang, D.; Sandoval, S. J.; Divigalpitiya, W. M. R.; Irwin, J. C.; Frindt, R. F. Structure of Single-Molecular-Layer MoS_2. *Phys. Rev. B: Condens. Matter Mater. Phys.* **1991**, *43*, 12053.
(13) Liu, X.; Zhang, Z.; Guo, W. Van der Waals Screening by Graphenelike Monolayers. *Phys. Rev. B* **2018**, *97*, 241411.
(14) Qiu, D. Y.; Felipe, H.; Louie, S. G. Optical Spectrum of MoS_2: Many-Body Effects and Diversity of Exciton States. *Phys. Rev. Lett.* **2013**, *111*, 216805.
(15) Erdemir, A.; Donnet, C. Tribology of Diamond, Diamond-like Carbon, and Related Films. *Modern Tribology Handbook*; Springer, 2001: Vol. *2*, pp 871−908.
(16) Berman, D.; Deshmukh, S. A.; Sankaranarayanan, S. K. R. S.; Erdemir, A.; Sumant, A. V. Extraordinary Macroscale Wear Resistance of One Atom Thick Graphene Layer. *Adv. Funct. Mater.* **2014**, *24*, 6640−6646.
(17) Gao, W.; Tkatchenko, A. Sliding Mechanisms in Multilayered Hexagonal Boron Nitride and Graphene: The Effects of Directionality, Thickness, and Sliding Constraints. *Phys. Rev. Lett.* **2015**, *114*, 096101.
(18) Kohn, W. Nobel Lecture: Electronic Structure of Matter−Wave Functions and Density Functionals. *Rev. Mod. Phys.* **1999**, *71*, 1253.
(19) Görling, A. Density-Functional Theory beyond the Hohenberg-Kohn Theorem. *Phys. Rev. A: At., Mol., Opt. Phys.* **1999**, *59*, 3359.
(20) Gonze, X.; Beuken, J.-M.; Caracas, R.; Detraux, F.; Fuchs, M.; Rignanese, G.-M.; Sindic, L.; Verstraete, M.; Zerah, G.; Jollet, F.; Torrent, M.; Roy, A.; Mikami, M.; Ghosez, P.; Raty, J.-Y.; Allan, D. C. First-Principles Computation of Material Properties: the ABINIT Software Project. *Comput. Mater. Sci.* **2002**, *25*, 478−492.
(21) Hamann, D. R. Optimized Norm-Conserving Vanderbilt Pseudopotentials. *Phys. Rev. B: Condens. Matter Mater. Phys.* **2013**, *88*, 085117.
(22) Perdew, J. P.; Burke, K.; Ernzerhof, M. Generalized Gradient Approximation Made Simple. *Phys. Rev. Lett.* **1996**, *77*, 3865.
(23) Grimme, S. Semiempirical GGA-Type Density Functional Constructed with A Long-Range Dispersion Correction. *J. Comput. Chem.* **2006**, *27*, 1787−1799.
(24) Shulenburger, L.; Baczewski, A. D.; Zhu, Z.; Guan, J.; Tománek, D. The Nature of the Interlayer Interaction in Bulk and Few-Layer Phosphorus. *Nano Lett.* **2015**, *15*, 8170−8175.
(25) Hybertsen, M. S.; Louie, S. G. Electron Correlation in Semiconductors and Insulators: Band Gaps and Quasiparticle Energies. *Phys. Rev. B* **1986**, *34*, 5390.
(26) Paillard, C.; Xu, B.; Dkhil, B.; Geneste, G.; Bellaiche, L. Photostriction in Ferroelectrics from Density Functional Theory. *Phys. Rev. Lett.* **2016**, *116*, 247401.
(27) Haleoot, R.; Paillard, C.; Kaloni, T. P.; Mehboudi, M.; Xu, B.; Bellaiche, L.; Barraza-Lopez, S. Photostrictive Two-Dimensional Materials in the Monochalcogenide Family. *Phys. Rev. Lett.* **2017**, *118*, 227401.
(28) Xia, F.; Wang, H.; Jia, Y. Rediscovering Black Phosphorus as An Anisotropic Layered Material for Optoelectronics and Electronics. *Nat. Commun.* **2014**, *5*, 4458.
(29) Rodin, A. S.; Carvalho, A.; Neto, A. C. Strain-Induced Gap Modification in Black Phosphorus. *Phys. Rev. Lett.* **2014**, *112*, 176801.
(30) Boulfelfel, S. E.; Seifert, G.; Grin, Y.; Leoni, S. Squeezing Lone Pairs: The A17 to A7 Pressure-induced Phase Transition in Black Phosphorus. *Phys. Rev. B: Condens. Matter Mater. Phys.* **2012**, *85*, 014110.
(31) Tran, V.; Soklaski, R.; Liang, Y.; Yang, L. Layer-Controlled Band Gap and Anisotropic Excitons in Few-Layer Black Phosphorus. *Phys. Rev. B: Condens. Matter Mater. Phys.* **2014**, *89*, 235319.
(32) Shu, H.; Li, Y.; Niu, X.; Wang, J. The Stacking Dependent Electronic Structure and Optical Properties of Bilayer Black Phosphorus. *Phys. Chem. Chem. Phys.* **2016**, *18*, 6085−6091.
(33) Lui, C. H.; Frenzel, A. J.; Pilon, D. V.; Lee, Y.-H.; Ling, X.; Akselrod, G. M.; Kong, J.; Gedik, N. Trion-Induced Negative Photoconductivity in Monolayer MoS_2. *Phys. Rev. Lett.* **2014**, *113*, 166801.
(34) Mate, C. M.; McClelland, G. M.; Erlandsson, R.; Chiang, S. *Scanning Tunneling Microscopy*; Springer, 1987; pp 226−229.
(35) Filleter, T.; McChesney, J. L.; Bostwick, A.; Rotenberg, E.; Emtsev, K. V.; Seyller, T.; Horn, K.; Bennewitz, R. Friction and Dissipation in Epitaxial Graphene Films. *Phys. Rev. Lett.* **2009**, *102*, 086102.
(36) Li, Y.; Guo, W. Spin Friction in Two-Dimensional Antiferromagnetic Crystals. *Phys. Rev. B* **2018**, *97*, 104302.

DOI: 10.1021/acsami.9b20285
ACS Appl. Mater. Interfaces XXXX, XXX, XXX−XXX

(37) Tománek, D.; Zhong, W.; Thomas, H. Calculation of An Atomically Modulated Friction Force in Atomic-Force Microscopy. *Europhys. Lett.* **1991**, *15*, 887.
(38) Socoliuc, A.; Bennewitz, R.; Gnecco, E.; Meyer, E. Transition from Stick-Slip to Continuous Sliding in Atomic Friction: Entering A New Regime of Ultralow Friction. *Phys. Rev. Lett.* **2004**, *92*, 134301.
(39) https://github.com/chenxin199261/MEPSearcher (accessed 2016).
(40) Cui, Z.; Xie, G.; He, F.; Wang, W.; Guo, D.; Wang, W. Atomic-Scale Friction of Black Phosphorus: Effect of Thickness and Anisotropic Behavior. *Adv. Mater. Interfaces* **2017**, *4*, 1700998.
(41) Kundys, B. Photostrictive Materials. *Appl. Phys. Rev.* **2015**, *2*, 011301.
(42) Lee, C.; Li, Q.; Kalb, W.; Liu, X. Z.; Berger, H.; Carpick, R. W.; Hone, J. Frictional Characteristics of Atomically Thin Sheets. *Science* **2010**, *328*, 76−80.
(43) Born, M.; Oppenheimer, R. Zur Quantentheorie der Molekeln. *Ann. Phys.* **1927**, *389*, 457−484.
(44) Hohenberg, P.; Kohn, W. Inhomogeneous Electron Gas. *Phys. Rev.* **1964**, *136*, B864.
(45) San-Jose, P.; Parente, V.; Guinea, F.; Roldán, R.; Prada, E. Inverse Funnel Effect of Excitons in Strained Black Phosphorus. *Phys. Rev. X* **2016**, *6*, 031046.
(46) Liu, X.-Z.; Ye, Z.; Dong, Y.; Egberts, P.; Carpick, R. W.; Martini, A. Dynamics of Atomic Stick-Slip Friction Examined with Atomic Force Microscopy and Atomistic Simulations at Overlapping Speeds. *Phys. Rev. Lett.* **2015**, *114*, 146102.
(47) Feng, J.; Qian, X.; Huang, C.-W.; Li, J. Strain-Engineered Artificial Atom as A Broad-Spectrum Solar Energy Funnel. *Nat. Photonics* **2012**, *6*, 866.
(48) Liu, X.; Guo, W. Shear Strain Tunable Exciton Dynamics in Two-Dimensional Semiconductors. *Phys. Rev. B* **2019**, *99*, 035401.
(49) Han, S. W.; Kwon, H.; Kim, S. K.; Ryu, S.; Yun, W. S.; Kim, D. H.; Hwang, J. H.; Kang, J.-S.; Baik, J.; Shin, H. J.; Hong, S. C. Band-Gap Transition Induced by Interlayer van der Waals Interaction in MoS_2. *Phys. Rev. B: Condens. Matter Mater. Phys.* **2011**, *84*, 045409.
(50) Li, Y.; Xu, L.; Liu, H.; Li, Y. Graphdiyne and Graphyne: From Theoretical Predictions to Practical Construction. *Chem. Soc. Rev.* **2014**, *43*, 2572−2586.
(51) Lin, Y.-M.; Dimitrakopoulos, C.; Jenkins, K. A.; Farmer, D. B.; Chiu, H.-Y.; Grill, A.; Avouris, P. 100-GHz Transistors from Wafer-Scale Epitaxial Graphene. *Science* **2010**, *327*, 662.
(52) Bunch, J. S.; Van Der Zande, A. M.; Verbridge, S. S.; Frank, I. W.; Tanenbaum, D. M.; Parpia, J. M.; Craighead, H. G.; McEuen, P. L. Electromechanical Resonators from Graphene Sheets. *Science* **2007**, *315*, 490−493.
(53) Hui, Y. Y.; Liu, X.; Jie, W.; Chan, N. Y.; Hao, J.; Hsu, Y.-T.; Li, L.-J.; Guo, W.; Lau, S. P. Exceptional Tunability of Band Energy in A Compressively Strained Trilayer MoS_2 Sheet. *ACS Nano* **2013**, *7*, 7126−7131.
(54) Kou, L.; Chen, C.; Smith, S. C. Phosphorene: Fabrication, Properties, and Applications. *J. Phys. Chem. Lett.* **2015**, *6*, 2794−2805.
(55) Kou, L.; Frauenheim, T.; Chen, C. Phosphorene as A Superior Gas Sensor: Selective Adsorption and Distinct I-V Response. *J. Phys. Chem. Lett.* **2014**, *5*, 2675−2681.

DOI: 10.1021/acsami.9b20285
ACS Appl. Mater. Interfaces XXXX, XXX, XXX−XXX